

# Dopant measurements in semiconductors with atom probe tomography

P. A. Ronsheim<sup>a)</sup> and M. Hatzistergos

IBM Semiconductor Research and Development Center, Hopewell Junction, New York 12533

S. Jin

Department of Materials Science, University of Florida, Gainesville, Florida 32611

(Received 22 June 2009; accepted 8 September 2009; published 3 March 2010)

The capability of atom probe tomography to make useful measurements of dopant distribution single device geometry is explored by characterizing the compositional accuracy of reconstructed data sets. The objective of this analysis is to evaluate whether atom probe can provide measurements to guide a predictive model development for diffusion in device geometry and strain conditions. Simple measurements of thin films of varying compositions show that, except for boron, all elements studied were collected and identified correctly and match secondary ion mass spectrometry reference values. Boron in silicon shows more variability and may require *in situ* concentration references. © 2010 American Vacuum Society. [DOI: 10.1116/1.3242422]

## I. INTRODUCTION

Laser-assisted atom probe tomography (APT) has demonstrated some success in analysis of materials used in semiconductor device fabrication, particularly with silicide formation and impurity segregation.<sup>1,2</sup> The nanometer-scale resolution and elemental sensitivity become useful characterization tools for materials science of semiconductors with potential to analyze individual devices. There have been some efforts to advance this capability<sup>3-5</sup> although several challenges remain before quantitative three dimensional device analyses are routine. A primary goal of the semiconductor analysis is to provide calibration measurements for predictive modeling of the lateral diffusion under the device edge. Atom probe tomography uses a voltage field to evaporate single ions using a pulsed field or later, allowing time-of-flight mass spectrometry to be performed on the ionized atoms, followed by a position-sensitive detector. Figure 1 is an APT reconstruction of a minority-carrier metal-oxide-semiconductor for field effect transistor (pFET) device, capturing the gate and channel regions, and illustrates the potential for device level characterization. Boron profiles extending under the spacer and the gate edge are extracted and vertical profiles can be normalized to one dimensional secondary ion mass spectrometry (SIMS) profiles from large planar structures of the boron implants on same wafer. SIMS has sub-nanometer depth scale accuracy for profiling impurity distributions in silicon, making it a strong reference to assess APT resolutions. This demonstrates that APT has the necessary capabilities for device level analysis, but the limitations need to be investigated. In the example of Fig. 1, the boron was normalized to SIMS measurements because the initial reconstruction concentrations in the body of polysilicon gate were low by a significant factor.

For current semiconductor manufacturing technology, the small devices have only several hundred impurity atoms distributed at the junction along the 50 nm width of the device.

Noting that the density of silicon is 50 at./nm<sup>3</sup> and the detector efficiency of APT is 50%, to measure a device junction at 5 × 10<sup>18</sup> at./cm<sup>3</sup> sensitivity with an atom probe, 400 nm<sup>3</sup>/data point would be needed. The lateral resolution of APT will be degraded when large volumes need to be summed to maintain the detection limit.

In device analysis, this can be overcome by using a device that is long on one side, allowing summing of the signal in the long axis. This type of structure is used for electrical characterization of the lateral dopant diffusion under the gate edge and is appropriate for the APT analysis.

A second limitation for APT in semiconductor device analysis is the inclusion of materials with differing field evaporation kinetics in the same sample volume. Features with higher evaporation fields will evaporate more slowly and result in tip radius uniformity problems which degrade the spatial reconstruction of the solid.<sup>6</sup> This is known as the local magnification effect and is shown in device cross sections with HfO<sub>2</sub> films between silicon layers. The HfO<sup>+</sup> evaporation is slower than the silicon, resulting in a non-spherical tip radius and distortions in positioning of the Hf atoms in the reconstruction. There are numerical models to both simulate the spatial distortions as well as attempt to make corrections.<sup>7,8</sup> Another approach to reducing the severity of this problem is to include features in the sample which can be measured independently, such as the gate polysilicon length or the HfO<sub>2</sub> thickness. This can prevent misinterpretation of the APT results. Additionally, the sample orientation can be optimized for the feature of interest, as better resolution data can be obtained by top-down orientation for film interfaces.

An important requirement for device measurements and model calibration with APT is the dose or composition accuracy. This will require calibration samples which can be used to assess the reconstruction spatial accuracy and composition calculations. Several parameters will need to be assessed including the reconstructed volume density and accurate mass peak assignments to account for all the dopant when ratios of molecular species can vary with tip temperature or laser

<sup>a)</sup>Electronic mail: ronsheim@us.ibm.com

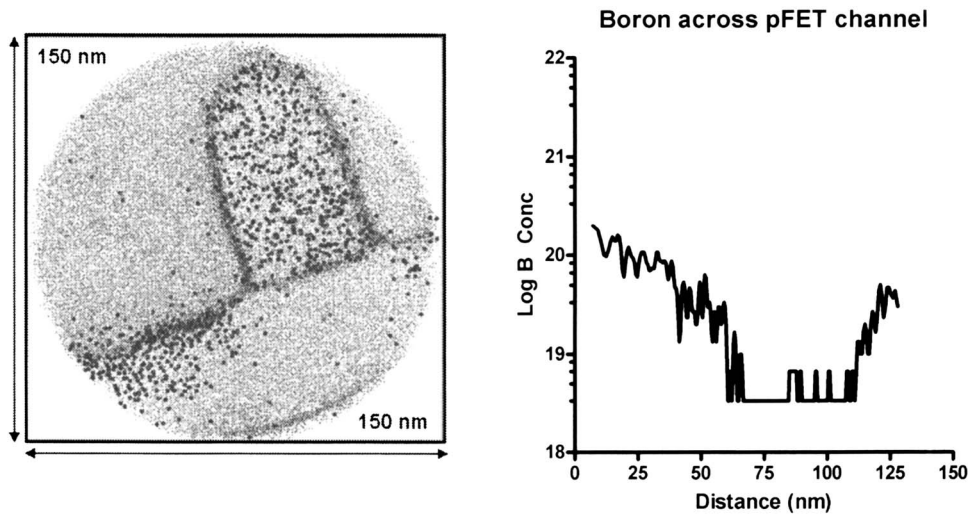


FIG. 1. Image on left is a reconstruction of the evaporated tip including a pFET device. Boron is represented with blue dots, oxygen with red, and silicon is gray. The overlying dielectric films were removed from the device and replaced with a deposited polycrystalline silicon. The film etching can potentially remove some surface silicon and associated boron atoms, however, TEM analysis indicates oxide remained on the Si surface, evidence that it was not attacked. A line profile of the boron concentration from the source under the channel to the drain is extracted a 10 nm wide strip under the gate and is plotted on the right. The boron concentration is normalized to a SIMS reference measurement of the vertical boron doping profile measured in a large planar structure adjacent to the device region; without this calibration the APT measured concentration is 70% lower than actual.

power. This article reviews recent experiments to determine the collection efficiency for B, As, P, C, and H in silicon using APT.

II. EXPERIMENT

The laser-assisted atom probe instrument used in this work is a LEAP3000X-Si, with a single wavelength (532 nm) laser. Boron detection efficiency is characterized using samples with varied boron concentrations and matrix compositions. The samples are boron doped polysilicon at  $2.15 \times 10^{20}$  B/cm<sup>3</sup>, and a low resistivity silicon substrate with a boron impurity level at  $2.4 \times 10^{19}$  at./cm<sup>3</sup>. Laser power, laser frequency, evaporation rate, and sample temperature were varied to assess instrumental parameter effects on boron evaporation and collection yield of boron and silicon.

A nominal  $2.5 \times 10^{15}$  As/cm<sup>2</sup> at 50 keV arsenic implant into silicon is used to characterize arsenic collection yield

TABLE I. APT arsenic dose measurements from a  $2.3 \times 10^{15}$  As/cm<sup>2</sup> implant showing consistent concentration measurements equivalent to the SIMS measured concentrations.

LEAP file	Arsenic dose $\times 10^{15}$ at./cm <sup>2</sup>
SIMS ref	2.34
53 112	2.26
53 145	2.24
53 157	2.17
53 161	2.31
Average	2.245
Std. dev.	0.06

while H, C, and P characterization was obtained from a silicon epitaxial deposition with carbon and phosphorus impurities. SIMS analysis with a Cameca IMS magnetic sector instrument was used to characterize the sample doping concentration, using NIST-traceable reference materials for the B, P, and As quantification. The arsenic dose was measured at  $2.34 \times 10^{15}$  As/cm<sup>2</sup> by SIMS referenced to the NIST SRM with a precision of 5%.

III. RESULTS

The arsenic implant dose measurements are shown in Table I. The variability between measurements is small and the collected arsenic to silicon ratio is consistent with the implant dose and the SIMS profile.<sup>9</sup> Other elemental species

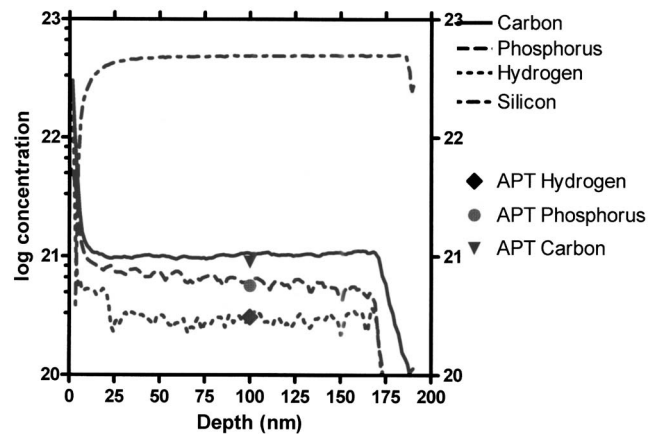


FIG. 2. SIMS depth profile of the Si:C:P epilayer on silicon with an overlay of the APT concentrations measured by the ratio of impurity to silicon. These elements show accurate concentration values without calibration to a standard.

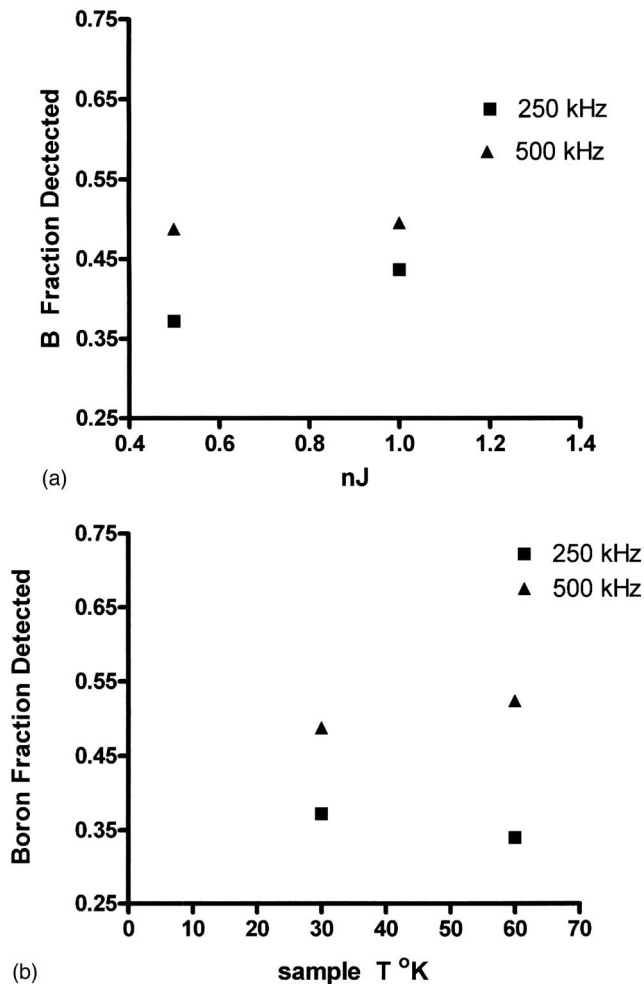


FIG. 3. (a) Boron fractional yield for two laser pulse frequencies of 250 and 500 kHz while varying the laser power from 0.5 to 1.0 nJ shows a modest improvement in collection efficiency at the higher pulse rate. The sample is the  $2.4 \times 10^{19}$  B/cm<sup>3</sup> bulk-doped single crystal silicon, held at 30° K with an evaporation rate of 0.2%. (b) Boron fractional yield at 0.5 nJ laser energy and 250 and 500 kHz against the sample temperature in degrees K. For this temperature range, there is no improvement in boron collection efficiency at higher temperatures. Evaporation rate is held to 0.2%.

with a similar mass/charge ratio as silicon were collected from a sample of an epitaxial silicon layer with hydrogen, carbon, and phosphorus incorporation. Figure 2 shows the SIMS depth profile with APT measured concentrations indicated. Again the APT concentrations determined from the atomic count ratios and demonstrate accuracy within 10% of the SIMS measurements; these are essentially equivalent concentration measurements given the precision of the methods.

Boron measurements are made on uniformly doped bulk silicon of  $2.4 \times 10^{19}$  B/cm<sup>3</sup>, and the LEAP experimental parameters of laser repetition rate, laser power, and sample temperature are varied. This sample is boron doped during crystal growth and has a low resistivity (0.01 Ω cm). The boron is expected to be fully dissolved or substitutional in the silicon lattice. Figure 3(a) plots the boron fractional detection for laser frequencies of 250 and 500 kHz against la-

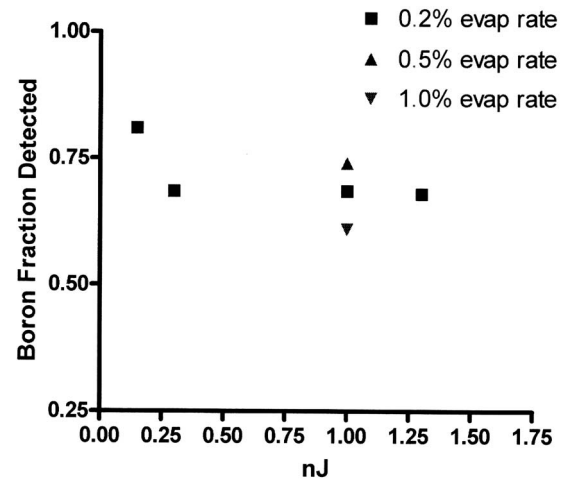


FIG. 4. Changing to the high concentration boron doped polysilicon sample shows increased collection efficiency for boron, but still not at 100%. Measurements for the square symbol were acquired at 30° K, 0.2% evaporation rate, and 250 kHz, the same as used for the low concentration single crystal sample. Boron fractional yield over laser power changes is shown here. Little change is observed with laser power with this sample. Additional data varying the evaporation rate are shown for the same conditions; increasing the evaporation rate requires an increase in the applied field for constant laser conditions. No trend in boron collection with evaporation rate is seen. The higher detection yield for this sample may be explained by the low count rates of the bulk-doped crystal sample.

ser power values of 0.5 and 1 nJ. A first observation is the boron collection efficiency is much lower than other species reported here. The higher laser pulse rate shows consistent increase in boron detected as does the laser power change. Figure 3(b) illustrates the effect of sample temperature on boron fractional yield—indicating no consistent trends for the two frequencies. The experiment to determine the dependence of boron detection on temperature is inconclusive. The B counting statistics on  $10 \times 10^6$  Si atom counts were weak, prompting this sample change, so a second sample with  $2.15 \times 10^{20}$  B/cm<sup>3</sup> in a polysilicon layer is used to allow higher count rates of boron. The boron yield is higher than on the single crystal material, however, the doped-polysilicon sample is quite different than the first boron material because of the presence of defects and grain boundaries in the silicon. Boron is expected to accumulate at these crystal boundaries and may cluster or have fewer silicon neighbors than the boron dissolved in the crystallites. Due to the higher number of boron atoms counted per silicon atom, the boron detection calculation is more accurate for this sample, but other mechanisms affecting the boron measurement could be occurring due to the defects in the silicon crystal. When laser power is varied from 0.5 to 1.5 nJ the measured boron fraction is nearly constant at 0.7 as shown in Fig. 4. Additionally, on Fig. 4, varying the evaporation rate does not show a consistent change in boron detection efficiency.

#### IV. DISCUSSION

Boron collection efficiency in a laser-assisted wide-angle atom probe can be much lower than the 100% observed with many other atomic species, including similarly low mass

species such as carbon and hydrogen. The observation from the initial experiments shown here is that higher laser power does not show a consistent trend while more frequent laser pulses can improve the boron collection. Sample temperature, evaporation rate, or boron concentration differences show no systematic trend.

The higher concentration boron-doped polysilicon sample shows significantly higher detected boron fraction than the low concentration single crystal sample. It is not clear why this should be, unless the low count rates on the bulk-silicon sample are distorting the results. This should be confirmed with longer atom collections at allow sufficient counting precision.

For an atom probe detector to “miss” or not detect a certain species, there must be some mechanism for that species to either not excite the detector or for that species to hit the detector while it is still counting an earlier event. The boron atom collection in the detector shows boron frequently evaporates as a “multiple” event, where more than one atom is detected for a laser pulse. If the multiple event occurs during a 3 ns interval after the first detected atom, it will not be detected. Boron may be more likely than other species to field evaporate if a neighboring Si atom evaporates with a laser pulse, thus coming to the detector just after the silicon arrival and prior to another laser pulse. Other elements with similar bonding to silicon could be investigated to develop this understanding.

## V. SUMMARY

Atomic collection efficiencies are seen to be uniform over many species important in semiconductor device analysis, with the exception of boron in silicon. Differences in evaporation mechanisms may result in undetected boron events. This example is investigated with variations in the atom probe laser power and sample temperature and indicates that a higher rate of laser pulsing can increase boron fractional yield. Other parameters such as laser power do not show a consistent trend in boron detection efficiency. Improvements in multiple event detection may correct this issue, however, further work is needed to verify the boron evaporation peculiarities.

<sup>1</sup>P. Adusumilli, L. J. Lauhon, D. N. Seidman, C. E. Murray, O. Avayu, and R. Rosenwaks, *Appl. Phys. Lett.* **94**, 113103 (2009).

<sup>2</sup>P. Ronsheim, J. McMurray, P. Flaitz, C. Parks, K. Thompson, D. Larson, and T. F. Kelly, *AIP Conf. Proc.* **931**, 129 (2007).

<sup>3</sup>M. J. Galtrey, R. A. Oliver, M. J. Kappers, C. J. Humphreys, P. H. Clifton, D. J. Larson, D. W. Saxey, and A. Cerezo, *J. Appl. Phys.* **104**, 013524 (2008).

<sup>4</sup>T. F. Kelly, D. J. Larson, K. Thompson, R. Alvis, J. H. Bunton, and B. Gorman, *Annu. Rev. Mater. Res.* **37**, 681 (2007).

<sup>5</sup>P. Ronsheim, P. Flaitz, M. Hatzistergos, C. Molella, K. Thompson, and R. Alvis, *Appl. Surf. Sci.* **255**, 1547 (2008).

<sup>6</sup>F. Vurpillot, A. Bostel, and D. Blavette, *Appl. Phys. Lett.* **76**, 3127 (2000).

<sup>7</sup>F. Vurpillot, A. Cerezo, D. Blavette, and D. J. Larson, *Microsc. Microanal.* **10**, 384 (2004).

<sup>8</sup>F. Vurpillot, D. Larson, and A. Cerezo, *Surf. Interface Anal.* **36**, 552 (2004).

<sup>9</sup>K. Thompson, P. Flaitz, P. Ronsheim, D. Larson, and T. F. Kelly, *Science* **317**, 1370 (2009).